Oligomerization and GTP-binding requirements of MxA for viral target recognition and antiviral activity against influenza a virus

Nigg, Patricia E ; Pavlovic, Jovan

Abstract: The IFN-induced human myxovirus resistance protein A (MxA) exhibits a broad antiviral activity against many viruses, including influenza A virus (IAV). MxA belongs to the family of dynamin-like GTPases and assembles in vitro into dimers, tetramers, and oligomeric ring-like structures. The molecular mechanism of action remains to be elucidated. Furthermore, it is not clear whether MxA exerts its antiviral activity in a monomeric and/or multimeric form. Using a set of MxA mutants that form complexes with defined stoichiometry, we observed that, in the presence of guanosine 5'-O-(thiotriphosphate), purified MxA disassembled into tetramers and dimers. Dimeric forms did not further disassemble into monomers. Infection experiments revealed that besides wild-type MxA, dimeric and monomeric variants of MxA also efficiently restricted IAV at a replication step after primary transcription. Moreover, only dimeric MxA was able to form stable complexes with the nucleoprotein (NP) of IAV. MxA interacted with NP independently of other viral components. Interestingly, the dimeric form of MxA was able to efficiently bind to NP from several MxA-sensitive strains but interacted much more weakly with NP from the MxA-resistant PR8 strain derived from the H1N1 1918 lineage. Taken together, these data suggest that, during infection, a fraction of MxA disassembles into dimers that bind to NP synthesized following primary transcription in the cytoplasm, thereby preventing viral replication.

DOI: https://doi.org/10.1074/jbc.M115.681494

THE JOURNAL OF BIOLOGICAL CHEMISTRY VOL. 290, NO. 50, pp. 29893–29906, December 11, 2015

Oligomerization and GTP-binding Requirements of MxA for Viral Target Recognition and Antiviral Activity against Influenza A Virus*

Received for publication, August 5, 2015, and in revised form, October 19, 2015 Published, JBC Papers in Press, October 27, 2015, DOI 10.1074/jbc.M115.681494

Patricia E. Nigg[1] **and Jovan Pavlovic**[2]

From the Institute of Medical Virology, University of Zürich, Winterthurerstrasse 190, 8057 Zürich, Switzerland

The IFN-induced human myxovirus resistance protein A (MxA) exhibits a broad antiviral activity against many viruses, including influenza A virus (IAV). MxA belongs to the family of dynamin-like GTPases and assembles *in vitro* into dimers, tetramers, and oligomeric ring-like structures. The molecular mechanism of action remains to be elucidated. Furthermore, it is not clear whether MxA exerts its antiviral activity in a monomeric and/or multimeric form. Using a set of MxA mutants that form complexes with defined stoichiometry, we observed that, in the presence of guanosine 5′-*O*-(thiotriphosphate), purified MxA disassembled into tetramers and dimers. Dimeric forms did not further disassemble into monomers. Infection experiments revealed that besides wild-type MxA, dimeric and monomeric variants of MxA also efficiently restricted IAV at a replication step after primary transcription. Moreover, only dimeric MxA was able to form stable complexes with the nucleoprotein (NP) of IAV. MxA interacted with NP independently of other viral components. Interestingly, the dimeric form of MxA was able to efficiently bind to NP from several MxA-sensitive strains but interacted much more weakly with NP from the MxA-resistant PR8 strain derived from the H1N1 1918 lineage. Taken together, these data suggest that, during infection, a fraction of MxA disassembles into dimers that bind to NP synthesized following primary transcription in the cytoplasm, thereby preventing viral replication.

The interferon system plays a pivotal role in the defense against viral infection. Interferons type I and III induce the expression of more than 300 proteins, many of them exhibiting intrinsic antiviral activity (1–3). The human myxovirus resistance protein A (MxA)[3] protein is induced exclusively by type I and type III interferons and restricts the replication of a large variety of RNA and DNA viruses (reviewed in Ref. 4). Mx proteins are members of the dynamin superfamily of large GTPases. They contain an amino-terminal globular GTPase (G) domain and a carboxy-terminal stalk domain (5, 6). The stalk domain harbors the GTPase effector domain and additional structural elements, including the L4 loop required for antiviral activity and target specificity (7–9). The G and stalk domains are connected via the bundle signaling element (BSE), which strongly resembles the BSE responsible for intramolecular signaling in dynamin (10). Mx proteins exhibit a high intrinsic rate of GTP hydrolysis, although the affinity to GTP is weak (11). Moreover, the human MxA protein forms dimers and tetramers and has the capacity to form higher oligomeric ring-like structures through a series of intra- and intermolecular interactions (5, 6, 12, 13). Introduction of mutations into the interfaces of the intermolecular interaction sites or hinge regions of MxA prevents assembly into higher-order multimeric forms. These mutations lead to the formation of MxA into tetramers, dimers, and monomers (5, 12).

So far, little is known about the molecular mechanism of action of the human MxA protein. Previous studies have demonstrated that GTP binding is required for its efficient antiviral activity against vesicular stomatitis virus and IAV (6, 14). In the case of IAV, several previous studies have demonstrated that ectopic expression of the nucleocapsid protein (NP) or the polymerase subunit 2 (PB2) of the virus partially abrogated the antiviral activity of mouse Mx1 (15–17). Moreover, human IAV strains are partially resistant to the activity of MxA, whereas non-adapted avian IAV strains such as H5N1 are highly sensitive to MxA. Recent findings indicate that resistance of human IAV strains to the activity of MxA is determined by NP (18). Adaptive mutations in a surface-exposed cluster of amino acids have been identified to counteract the restriction by MxA (19, 20). So far, there is only little evidence for a physical interaction between NP of IAV and MxA (21). We have shown recently that MxA binds to UAP56, a DEAD-box helicase. UAP56 is also an interaction partner of NP and is required for efficient replication of IAV and evasion of the IFN response (22–24). Therefore, UAP56 may recruit MxA and NP to form a complex involving all three proteins.

To date, it is not clear whether the assembly of MxA into higher-ordered oligomeric structures is required to confer antiviral activity. Several previous studies have revealed that a monomeric mutant of MxA (L612K) still exhibited a pronounced antiviral activity against IAV and Thogotovirus and vesicular stomatitis virus (6, 25–27). On the basis of these findings, we previously proposed a model where newly synthesized MxA

* This work was funded by Schweizerischer Nationalfonds zur Förderung der Wissenschaftlichen Forschung Grant 31003A_143834. The authors declare that they have no conflicts of interest with the contents of this article.

[1] Present address: Friedrich Miescher Institute for Biomedical Research, Maulbeerstr. 66, 4002 Basel, Switzerland.

[2] To whom correspondence should be addressed: Institute of Medical Virology, University of Zurich, Winterthurerstr. 190, 8057 Zurich, Switzerland. Tel.: 41-44-634-2656; E-mail: pavlovic.jovan@virology.uzh.ch.

[3] The abbreviations used are: MxA, myxovirus resistance protein A; BSE, bundle signaling element; IAV, influenza virus A; NP, nucleoprotein; vRNP, viral ribonucleoprotein; GTPγS, guanosine 5′-3-*O*-(thio)triphosphate; FPV, fowl plague virus; AMP-PNP, adenosine 5′-(β,γ-imino)triphosphate; SEC-MALS, size exclusion chromatography and multi-angle light scattering; $TCID_{50}$, 50% tissue culture infective dose.

would assemble into higher-ordered oligomeric, preactivated structures and would disassemble into antivirally active monomers in response to a viral trigger in infected cells (6). On the other hand, on the basis of the recently solved crystal structure of MxA, Gao *et al.* (5, 12) proposed a model where MxA would assemble into ring-like structures around incoming viral ribonucleoprotein (vRNP) complexes. These ring-like structures would then interfere with nuclear import and/or primary transcription. However, previous studies with stable MxA-expressing cell lines have clearly demonstrated that MxA inhibits an as yet undefined cytoplasmic step of the IAV life cycle that follows primary transcription (28).

To clarify this issue, we first evaluated *in vitro* the influence of GTP binding on the assembly state of MxA and assessed various interface and hinge mutants with defined monomeric or multimeric forms for their antiviral activity and capacity to interact with NP of IAV. The data indicate that, in the presence of GTPγS, recombinant MxA disassembles from higher-ordered oligomeric structures into tetramers and dimers. Contrary to previous reports by Gao et al. (5, 12), dimeric and monomeric forms of MxA also exerted a pronounced antiviral activity against avian IAV. Furthermore, only MxA in its dimeric form was able to form stable complexes with NP deriving from MxA-sensitive IAV strains independent of other viral components.

Experimental Procedures

Cells and Viruses—Madin-Darby canine kidney cells, African green monkey kidney (Vero) cells, HeLa cells, and HEK293T cells (all from the ATCC, LGC Standards) were cultured in growth medium consisting of Dulbecco's modified Eagle's medium supplemented with 10% FCS, 1× Glutamax, and 1× penicillin/streptomycin (Invitrogen). Cells transiently expressing human MxA (wild type or variants) were generated by transfecting the cells with pcDNA3.1(+)neo constructs coding for MxA wild-type or mutant using JetPRIME (Polyplus Transfection) according to the protocol of the manufacturer.

All infection experiments were carried out using A/Puerto Rico/8/1934(H1N1) (PR8), pH1N1-NP(H5N1), A/seal/Mass/1/1980(H7N7) (mouse-adapted mutant rSC35M), or A/FPV/Dobson/1927(H7N7) (FPV). PR8, rSC35M, and FPV were prepared from supernatants of virus-infected Madin-Darby canine kidney cells. The reassortant virus pH1N1-NP(H5N1) was provided by Martin Schwemmle and has been published before (18). For infection, cells were kept in infection medium (Dulbecco's modified Eagle's medium supplemented with 20 mM Hepes, 0.2% BSA, 1× Glutamax, and 1× penicillin/streptomycin (Invitrogen)). Unless indicated otherwise, cells were maintained at 37 °C in 5% CO_2.

Plasmid Construction—The coding sequence of the MxA cDNA used has been described previously (29). The cDNAs of the MxA mutants MxA(T103A), MxA(R640A), MxA(L617D), and MxA(M527D) have been described previously (5, 12, 26) (provided by Georg Kochs, Freiburg, Germany) and were introduced into the expression plasmids pQE30 (Qiagen) and pcDNA3.1(+)neo (Invitrogen). The expression vectors for Mx1 and Mx1(K49A) have been described previously (11).

Purification of His-tagged Recombinant Human MxA—400 ml of LB medium supplemented with 0.1% glucose, 100 μg/ml ampicillin, and 50 μg/ml kanamycin was inoculated with *Escherichia coli* DH5α transformed with pQE30-MxA (wild type or variant) at an A_{600} of 0.1. The expression cultures were incubated at 37 °C and 180 rpm until an A_{600} of 0.4–0.6 was reached. The expression cultures were cooled to 19 °C and induced with 45 μM isopropyl-β-D-thiogalactopyranoside. At 19 °C and 180 rpm, the expression cultures were incubated overnight. For harvesting, the expression cultures were centrifuged at 5000 × *g* and 4 °C. The pellet was resuspended in lysis buffer (50 mM Hepes (pH 7.5), 500 mM NaCl, 5 mM $MgCl_2$, 0.5% CHAPS, 5 mM β-mercaptoethanol, 30 mM imidazole, Roche Complete protease inhibitor mixture, and 1 mg/ml lysozyme) and sonicated for 6 cycles of 10 pulses on ice. After centrifugation at 15,000 × *g* and 4 °C, the soluble fraction was filtered (pore size, 0.2 μm) and incubated with lysis buffer equilibrated with nickel-nitrilotriacetic acid Superflow (Qiagen) overnight at 4 °C on a rotating wheel. The protein-loaded nickel-nitrilotriacetic acid was washed with 5 volumes of wash buffer I (50 mM Hepes (pH 7.5), 800 mM NaCl, 5 mM $MgCl_2$, 0.5% CHAPS, 5 mM β-mercaptoethanol, 1 mM ATP, and 30 mM imidazole) and 5 volumes of wash buffer II (50 mM Hepes (pH 7.5), 200 mM KCl, 5 mM $MgCl_2$, 0.5% CHAPS, 5 mM β-mercaptoethanol, and 80 mM imidazole). The His-tagged protein was eluted with 2.5 volumes of elution buffer (50 mM Hepes (pH 7.5), 200 mM KCl, 5 mM $MgCl_2$, 0.5% CHAPS, 5 mM β-mercaptoethanol, and 300 mM imidazole), and, subsequently, the buffer was exchanged with storage buffer (50 mM Hepes (pH 7.5), 200 mM KCl, 5 mM $MgCl_2$, 5 mM β-mercaptoethanol, and 20% glycerol) using disposable PD-10 desalting columns (GE Healthcare Biosciences) according to the protocol of the manufacturer. The samples were stored at −80 °C until further analysis.

GTPase Activity Analysis of Recombinant Human MxA—The GTPase activity of purified recombinant MxA was determined by incubating 0.01, 0.1, 1, 10, and 100 μg/ml purified recombinant MxA sample with 10 μM GTP and 0.1 μM AMP-PNP at 37 °C for 1 h. The sample was analyzed using the Transcreener GDP assay (Belbrooks Lab) according to the manual of the manufacturer. The GTPase activity was normalized to 100% GDP conversion by incubating the reaction mixture with 10 μM GDP instead of GTP.

Size Exclusion Chromatography and Multi-angle Light Scattering (SEC-MALS)—Purified recombinant human MxA samples were dialyzed against 50 mM Hepes (pH 7.5), 200 mM KCl, 5 mM $MgCl_2$, and 0.75 mM DTT overnight. Then 1 mg/ml purified recombinant human MxA samples were incubated with either 1 mM GTPγS or buffer at 37 °C for 1 h prior to analysis by SEC-MALS. To determine the exact molar mass of each recombinant human MxA construct, SEC-MALS measurements were performed as follows. 100 μl of the sample was loaded on a 24-ml Superdex 100 column (GE Healthcare Biosciences) with a flow rate of 0.5 ml/min and 50 mM Hepes (pH 7.5), 200 mM KCl, 5 mM $MgCl_2$, and 0.75 mM DTT as running buffer. The chromatograph was calculated according to the UV absorbance (280 nm). The SEC was followed by miniDAWN three-angle light-scattering detector (Wyatt Technology) and Optilab rEX differential refractometer (Wyatt Technology) analyses. The

calculation of the molar mass was determined by the scattered light (Rayleigh ratio) measured by the MALS detector. The data were recorded and analyzed using the ASTRA V software (Wyatt Technology).

Split-GFP Complementation Assay—The cloning of the vectors pCDNA3.1-GFP(158–238) and pCDNA3.1-GFP(1–157) has been described before (30). To clone the MxA wild type and variants in either of these vectors, the open reading frames of those constructs were amplified using PCR and subsequently introduced into the multiple cloning site located at the C terminus of the GFP fragment. HeLa cells were transfected with these constructs using Viafect (Promega) according to the protocol of the manufacturer. 24 h post-transfection, cells were incubated at 27 °C for 2 h before fixation with 3% paraformaldehyde. After permeabilization with 0.5% Triton X-100, cells were stained with a mouse monoclonal MxA antibody (HB143 supernatant, in-house). Samples were mounted in DAPI containing mounting medium (Fluoromount, Southern Biotech) and consequently analyzed by confocal laser-scanning microscopy (CLSM Leica SP5, Leica Microsystems) using the LAS AF software (Leica).

Non-denaturing PAGE—Non-denaturing PAGE was performed as described before with a few modifications (31). Basically, Vero cells were grown in 10-cm dishes and transfected with MxA coding plasmids. Cells were lysed (20 mM Tris-HCl (pH 7.5), 150 mM NaCl, 5 mM $MgCl_2$, 100 μM iodoacetamide, 50 mM NaF, 1 mM Na_3VO_4, 1% Nonidet P-40, 50 mM β-glycerophosphate, and Roche Complete protease inhibitor mixture) in the dark on ice for 30 min. To remove cell debris, lysates were centrifuged at 13,000 $\times$ *g* for 20 min at 4 °C. As described for blue native PAGE (32), lysates were dialyzed against 20 mM Tris-HCl (pH 6.8), 10% glycerol, 0.1% CHAPS, and 0.5 mM DTT at 4 °C for 4 h using Slide-A-Lyzer MINI dialysis devices with a 10,000 cutoff (Thermo Scientific). Dialyzed samples were centrifuged at 13,000 $\times$ *g* and 4 °C for 20 min before loading on a precast 4–16% TGX™ gradient gel (Bio-Rad). Using 25 mM Tris-HCl (pH 8.3), 192 mM glycine, 0.5 mM DTT, and 0.1% CHAPS as running buffer, the gel was run at 4 °C with a constant current of 25 mA for 4 h. The gel was incubated in 25 mM Tris-HCl (pH 8.3), 192 mM glycine, and 0.1% SDS for 10 min before Western blotting. Blots were stained for MxA (rabbit anti-Mx1, Novus Biologicals, catalog no. H00004599_D01P). The molecular weight was determined using nativeMARK (Invitrogen).

Assay for Antiviral Activity ($TCID_{50}$ per Milliliter)—The 50% tissue culture infective dose ($TCID_{50}$) was determined by infection of HEK293T cells transiently expressing MxA (wild type or variants) with a 10-fold serial dilution of pH1N1-NP(H5N1) (virus stock, 1.64×10^8 $TCID_{50}$/ml) at 37 °C for 24 h. Cells were immunostained for NP using HB65 supernatant (ATCC). The $TCID_{50}$ per milliliter was calculated according to the method by Reed and Muench (47).

Minimal Replicon Reconstitution Assay—The minimal replicon reconstitution assay has been described before (33). In a 24-well dish, HEK293T cells were co-transfected with 10 ng of pcaggs-PB1, 10 ng of pcaggs-PB2, 10 ng of pcaggs-PA, 50 ng of pcaggs-NP, and 50 ng of pPolI-FFluc-RT firefly luciferase flanked by the non-coding regions of segment 8 of influenza A virus using JetPEI (Polyplus Transfection). Also included in the transfection mixture were 100 ng of the constitutively *Renilla*-expressing plasmid pRL-SV40. Additionally, 200, 400, or 800 ng of pcDNA3.1(+)neo MxA was added. To maintain constant DNA levels, empty vector (pcDNA3.1(+)neo) was included in the reaction mixture. All viral constructs were derived from the A/Thailand/1/2004 (Kan-1) strain. 24 h post-transfection, cells were assayed for luciferase activity using the Dual-Luciferase assay (Promega). Transfection efficiency was normalized by the *Renilla* luciferase signal.

In the case of NP and PB2 plasmid titration, the amounts of plasmids encoding MxA (200 ng) and mouse Mx1 (45 ng) were kept constant, whereas the amounts for the PB2 and NP coding plasmids were increased gradually (NP: 50, 100, 200, 400, 800, or 1600 ng; PB2: 10, 20, 40, 80, 160, or 320). To maintain a constant amount of transfected DNA, empty pcDNA3.1(+)neo was used.

RT qPCR—HEK293T cells transiently expressing MxA (wild type or variants) were grown in 6-well dishes and pretreated with 10 μM cycloheximide or solvent for 1 h at 37 °C before infection with either pH1N1-NP(H5N1) or PR8 at m.o.i. 5 for 6 h. Total RNA was purified as follows. Cells were lysed in 500 μl of TRIzol reagent (Invitrogen). 100 μl of chloroform was added to the lysates, mixed, and centrifuged at 13,000 $\times$ *g* for 15 min at 4 °C. After centrifugation, 600 μl of the aqueous RNA-containing phase was mixed with 600 μl of 70% EtOH. The resulting solution was transferred onto RNeasy spin columns (Qiagen), and further RNA extraction steps were performed according to the RNeasy Mini Kit protocol (Qiagen). cDNA was synthesized using SuperScript III reverse transcriptase (Life Technologies) according to the protocol of the manufacturer, using oligo(dT)15 (Promega) as a primer. PB2 and GAPDH transcripts were detected in an EvaGreen® (Biotum)-based qPCR reaction (denaturation, 95 °C and 15 s; annealing and extension, 60 °C and 60 s). The primers for PB2 were as follows: forward, 5-GCAGAACCCAACAGAAGAGC; reverse, 5-GCTGTTGCTCTTCTCCCAAC. The primers for GAPDH were as follows: forward, 5-CTGGCGTCTTCACCACCATGG; reverse, 5-CATCACGCCACAGTTTCCCGG. The -fold change ($2^{-\Delta\Delta Ct}$) was calculated according to Pfaffl (34). Expression levels were analyzed using Western blotting. Blots were immunostained using the following antibodies: monoclonal mouse anti-MxA (35), monospecific rabbit anti-Mx1 (36), polyclonal rabbit anti-NP,[4] and polyclonal rabbit anti-GAPDH (Santa Cruz Biotechnology, catalog no. sc-25778).

vRNP Import Assay—Vero cells were transfected with either pcDNA3.1(+)neo MxA or empty vector using Viafect (Promega). 24 h post-transfection, cells were pretreated with 10 μM cycloheximide or solvent for 1 h at 37 °C. Then cells were infected with FPV at m.o.i. 10 for 4 h in the presence of cycloheximide or solvent. Cells were fixed with 3% paraformaldehyde and permeabilized using 0.5% Triton X-100. Cells were stained using an affinity-purified polyclonal MxA antibody (derived from rabbit serum against recombinant His-MxA) and a monoclonal NP antibody (catalog no. HB65, ATCC). Samples

[4] D. A. Müller and J. Pavlovic, unpublished data.

were mounted in DAPI containing mounting medium (Fluoromount, Southern Biotech) and consequently analyzed by confocal laser-scanning microscopy (CLSM Leica SP5, Leica Microsystems) using LAS AF software (Leica). Images were assessed for nuclear import of vRNPs by counting MxA-expressing cells with a nuclear NP signal. Additionally, the NP mean nuclear signal intensity of MxA-expressing cells was analyzed using ImageJ software. Cells not expressing MxA were used as a negative control for both analyses.

Co-immuno-precipitation—Co-immunoprecipitation was either performed with pH1N1-NP(H5N1)- or rSC35M-infected (m.o.i. 5) Vero cells transiently expressing MxA (wild type or mutant) for 6 h or Vero cells co-transfected with pcaggs-NP (Kan-1, pH1N1, or PR8) and pcDNA3.1(+) neo-MxA (wild type or variant). In either case, cells were lysed (20 mM Tris-HCl (pH 7.5), 150 mM NaCl, 5 mM $MgCl_2$, 100 nM iodacetamide, 50 mM NaF, 1 mM Na_3VO_4, 1% Nonidet P-40, 50 mM β-glycerophosphate, and Roche Complete protease inhibitor mixture) for 30 min in the dark on ice. Lysates were transferred on QiaShredder columns (Qiagen) and subsequently centrifuged in a tabletop centrifuge at 13,000 $\times$ *g* for 20 min at 4 °C. IAV NP was immunoprecipitated from lysates with 0.5 μg of anti-NP (HB65 supernatant, ATCC) on a rotating wheel at 4 °C overnight. To capture the complexes, magnetic protein G Dynabeads (Invitrogen) were blocked with lysates of untreated cells and then incubated with the immunoprecipitated lysates on the rotating wheel for 3 h at 4 °C. Beads were washed six times in washing buffer (20 mM Tris-HCl (pH 7.5), 150 mM NaCl, 5 mM $MgCl_2$, and 1% Nonidet P-40) while vortexing. Bound protein was eluted in Laemmli buffer at 92 °C for 5 min. Samples were analyzed by SDS-PAGE and Western blot analysis. Blots were stained for MxA (rabbit anti-Mx1, Novus Biologicals, catalog no. H00004599_D01P), NP (rabbit anti-NP, in-house), and GAPDH (rabbit anti-GAPDH, Santa Cruz Biotechnology, catalog no. sc-25778).

Results

Oligomeric MxA Disassembles upon GTP Binding into Tetramers and Dimers—To investigate whether MxA has to first adopt a defined oligomeric or monomeric form to exert antiviral activity against IAV, we made use of several mutants of MxA that form complexes with a defined stoichiometry (Fig. 1*A*) (5, 12). First, we assessed whether GTP binding has an influence on the oligomerization of recombinant wild-type MxA and MxA interface mutants (Fig. 1*A*) using SEC-MALS analysis. For this purpose, recombinant His-tagged MxA proteins were expressed in bacteria and subsequently affinity-purified using nickel-agarose columns. The purification was monitored by SDS-PAGE and Coomassie staining (Fig. 1*B*). The activity of the purified proteins was then tested by measuring their GTPase activity in dependence of their concentration (Fig. 1*C*). With the exception of the G domain mutant MxA(T103A), wild-type MxA as well as the MxA mutants forming complexes with defined stoichiometry exhibited GTPase activity in a very similar manner, as described in previous reports (5, 12). Subsequently, the oligomeric state of the purified MxA protein complexes was assessed by SEC-MALS analysis in the presence or absence of the non-hydrolysable GTP analog GTPγS (Fig. 1*D*). In the presence of 1 mM GTPγS, wild-type MxA disassembled from higher-ordered oligomeric structures to tetramers and, to a small extent, also to dimers. The hinge 1 mutant MxA(R640A) shifted from a tetrameric to a dimeric state. By contrast, in the presence of GTPγS, the stalk interface 1 and 2 mutants, dimeric MxA(L617D), and monomeric MxA(M527D) did not alter their stoichiometries (Fig. 1*D*). These data clearly demonstrate that GTP binding induced purified MxA to disassemble from higher oligomeric structures to tetramers and dimers. Similar data have been obtained previously for dynamin. Under low-salt conditions and in the presence of GTPγS, preassembled dynamin is destabilized, forming lower oligomeric structures (37). As expected, the addition of GTPγS did not lead to a stable dimerization of the monomeric MxA(M527D) via the G domain.

Oligomeric MxA Accumulates in the Perinuclear Region of Mammalian Cells—To assess whether the oligomerization of MxA occurs at defined subcellular sites, we carried out the split-GFP complementation assay as described previously using HeLa cells and concomitantly immunostained MxA with a specific antibody (30). As expected, pairwise co-transfection of constructs encoding split-GFP-MxA fusion proteins of wild-type MxA, MxA(R640A), and MxA(L617D) led to pronounced GFP signals indicative of the formation of dimers or higher-ordered oligomers, whereas co-transfection of the constructs encoding the split-GFP-MxA fusion proteins of the monomeric variant MxA(M527D) did not exhibit any GFP signal. Wild-type MxA, MxA(R640A), and MxA(L617D) accumulated in a pronounced punctuate pattern in the perinuclear region (Fig. 2*A*). Parallel immunostaining of the split-GFP-MxA fusion proteins with an MxA-specific antibody revealed an identical distribution of the MxA and GFP signals. This observation indicates that a very high percentage of the fusion proteins is engaged in oligomeric structures. The MxA-specific staining of split-GFP-MxA (M527D) fusion protein revealed a diffuse, predominantly perinuclear localization (Fig. 2*A*). Immunostaining of an untagged version of wild-type MxA and MxA mutants expressed in Vero cells revealed a more dispersed distribution of MxA in the cytoplasm. Because split-GFP complexes have to be stabilized by incubation at 27 °C for 2 h to yield a detectable signal, we also incubated the untagged version of MxA under these conditions before fixation. This led to a pronounced accumulation of MxA in dot-like structures (Fig. 2*A*). Therefore, it is conceivable that the observed punctuate pattern of the split-GFP-MxA fusion proteins is, at least in part, the result of incubation at 27 °C. As reported previously, no significant MxA immunostaining or GFP-MxA signal was detected in the nuclei (Fig. 2*A*) (6, 30).

In the next step, we assessed which stoichiometry wild-type MxA and its interface or hinge 1 variants adopt in mammalian cells using gel electrophoresis under non-denaturing conditions. For this purpose, Vero cells were transfected with expression vectors encoding wild-type MxA, MxA(R640A), MxA (L617D), MxA(M527D), and the GTPase-deficient MxA(T103A). After 24 h, the cells were lysed under non-denaturing conditions, and the lysates were subjected to non-denaturing PAGE and Western blot analysis using an MxA-specific antibody (Fig. 2*B*). The results revealed that most of the wild-type MxA ran at a molecular mass of ~300 kDa, indicating that it predominantly

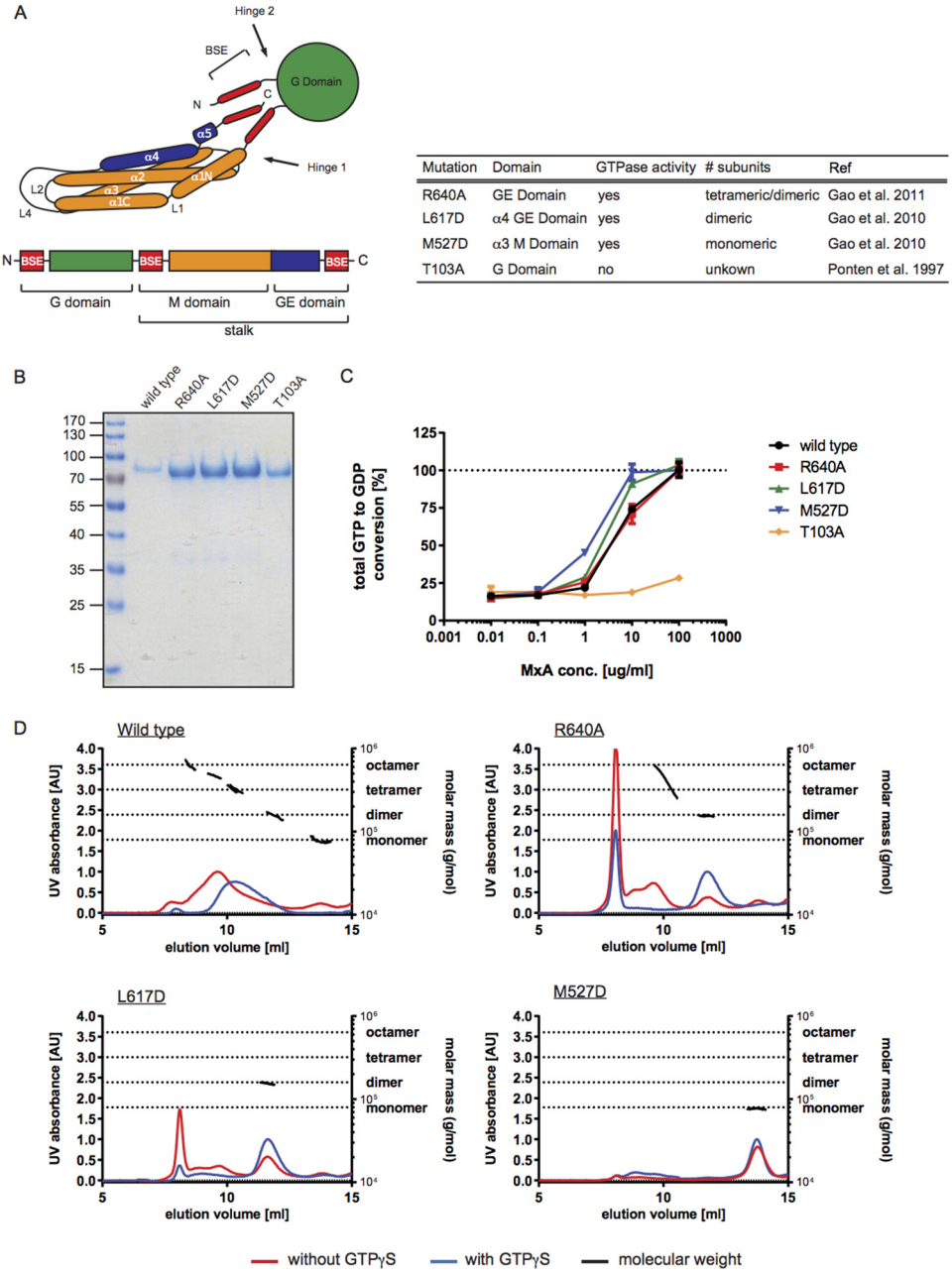

Mutation	Domain	GTPase activity	# subunits	Ref
R640A	GE Domain	yes	tetrameric/dimeric	Gao et al. 2011
L617D	α4 GE Domain	yes	dimeric	Gao et al. 2010
M527D	α3 M Domain	yes	monomeric	Gao et al. 2010
T103A	G Domain	no	unkown	Ponten et al. 1997

FIGURE 1. **Purified human MxA disassembles into tetramers and dimers in the presence of GTPγS.** *A*, schematic of the human MxA structure on the basis of its crystal structure (5, 12). The GTPase (*G*), middle (*M*), and GTPase effector (*GE*) domains; BSE; and interface and hinge regions are depicted. The stalk region comprises the middle and GTPase effector domains as well as two entities of the BSE. Listed are the mutations affecting the stoichiometry or GTPase activity of human MxA. *B*, Coomassie-stained SDS-PAGE gel of purified His-tagged wild-type MxA and the indicated mutants with defined stoichiometry. *C*, GTPase activity of the MxA wild type and the indicated mutants in dependence of their concentration (*conc.*). Data are represented as mean ± S.E. of duplicates. *D*, analysis of self-assembly of purified wild-type MxA, MxA(R640A), MxA(L617D), and MxA(M527D) by MALS combined with size exclusion chromatography. Elution profiles of the recombinant MxA proteins were monitored by absorption at 280 nm. Samples were analyzed in the absence (*red line*) or presence of 1 mM GTPγS (*blue line*). The absolute molecular weights are depicted as *black lines*. The graphs are representative of two independent experiments. *AU*, absorbance unit.

formed tetramers. Interestingly, MxA(T103A) deficient for GTP-binding and hydrolysis also ran as a tetramer, suggesting that, in mammalian cells, MxA assumes a tetrameric form independent of GTP binding. The hinge 1 mutant MxA(R640A), however, which exhibited a molecular mass of ~140 kDa, appeared to assemble into dimers. This contrasted with our observation made with purified MxA(R640A), which assembled primarily into tetramers in the absence of GTPγS (Fig. 1*D*). As expected, the interface variants MxA(L617D) and MxA(M527D) accumulated as dimers and monomers, respectively (Fig. 2*B*). MxA from lysates of IFN-induced A549 cells also separated as tetramers, indicating that the stoichiometry of ectopically expressed MxA protein complexes is comparable with the endogenous protein (Fig. 2*B*). Incubation of extracts of MxA-expressing cells with 1 mM GTP or GTPγS for 1 h at 4 °C before separation on denaturing PA gels had no influence on the stoichiometry of MxA. Incubation at higher temperatures (25 °C or 37 °C) led to a rapid degradation of MxA despite the presence of

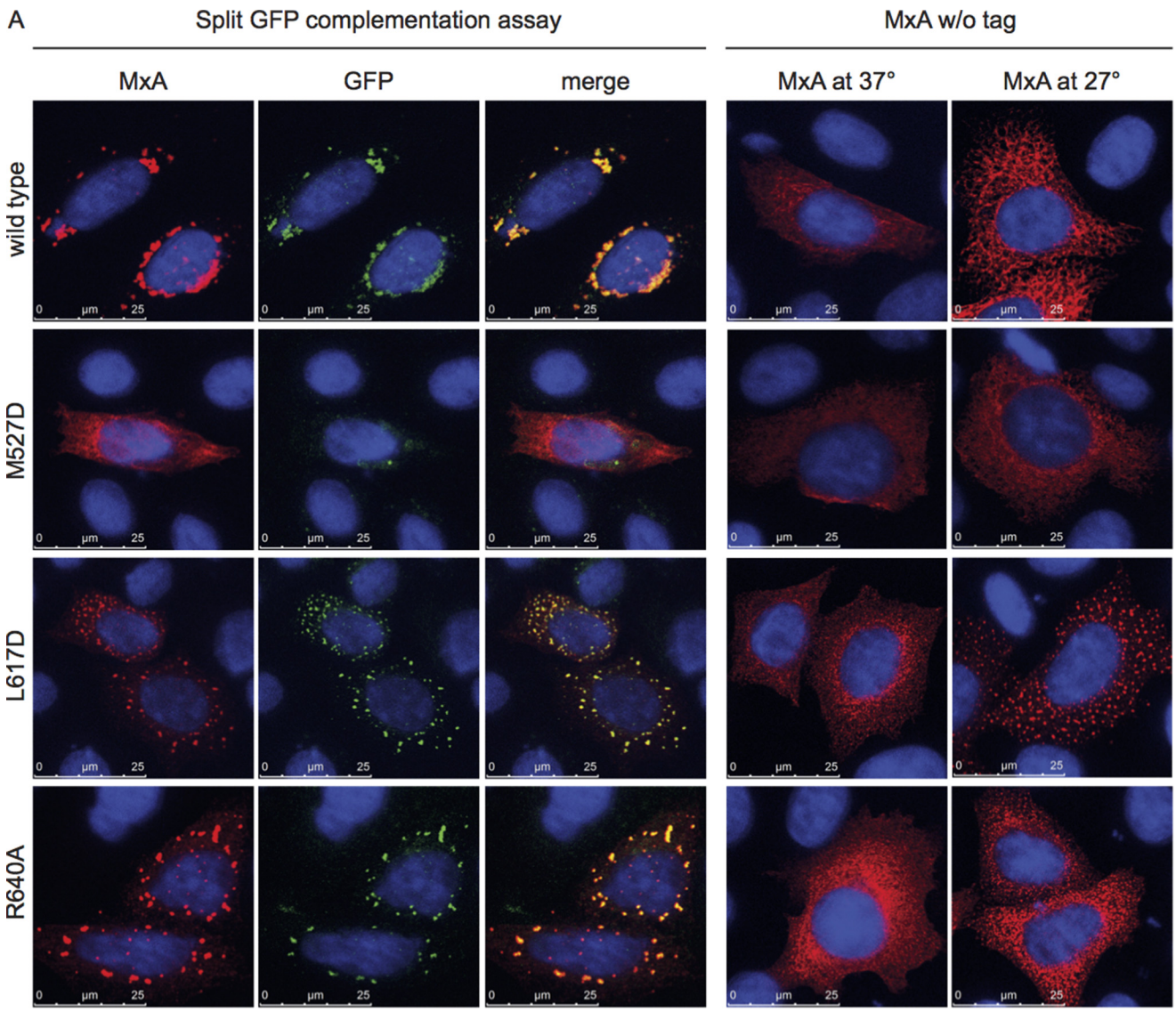

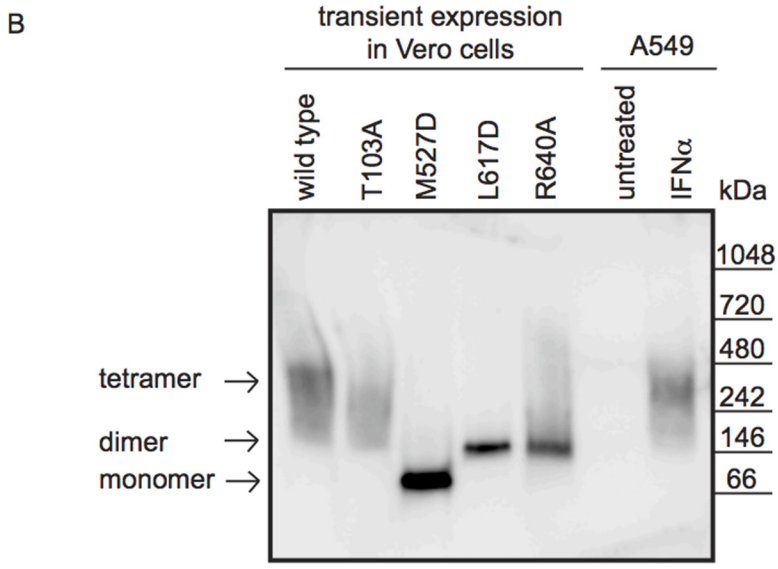

a high concentration of protease inhibitors (data not shown). Therefore, when expressed in mammalian cells, wild-type MxA, and in particular also the hinge 1 mutant MxA(R640A), adopted a similar stoichiometry as purified recombinant MxA incubated with GTPγS.

MxA Interface and Hinge 1 Mutants Exert Antiviral Activity against IAV in a Dose-dependent Manner—In the next step, we evaluated whether the MxA interface and hinge 1 variants restricted IAV infection. For this purpose, we transfected HEK293T cells with plasmids encoding wild-type MxA, the interface variants MxA(L617D) (dimer) and MxA(M527D) (monomer), and the hinge 1 variant MxA(R640A) (dimer/tetramer) as well as the inactive MxA(T103A) and infected them with the MxA-sensitive IAV strain pH1N1-NP (H5N1) at various concentrations (18). The virus titer was determined by measuring the $TCID_{50}$ per milliliter directly on the cells expressing wild-type MxA or MxA mutants, as outlined under "Experimental Procedures." Wild-type MxA as well as all interface and hinge 1 mutants exhibited a pronounced inhibition of IAV growth (~90%) compared with cells expressing the inactive mutant MxA(T103A) (Fig. 3*A*). MxA expression control of the transfected cells, depicted in Fig. 3*B*, showed that the antivirally active variants of MxA were not expressed at higher levels than the positive and negative controls, wild-type MxA and MxA(T103A), respectively. In addition, we tested the antiviral activity of MxA complexes with defined stoichiometry using the plasmid-based IAV minimal replicon reconstitution assay of the A/Thailand/1/2004 (Kan-1) strain (Fig. 3*C*) (18). To that end, we co-transfected plasmids encoding the components of the viral replicase, the virus-dependent luciferase reporter gene, and increasing amounts of MxA-encoding plasmids (200, 400, and 800 ng of plasmid). The data clearly showed that the tested MxA stalk interface 1 and 2 mutants as well as the BSE hinge 1 variant strongly restricted the amplification of the luciferase reporter gene in an expression level-dependent manner, whereas MxA(T103A) had no effect, even at high expression levels (Fig. 3, *C* and *D*). As reported previously (8, 12), the stalk interface 3 mutant MxA(R408A) and MxA lacking the L4 loop MxA(ΔL4) showed no antiviral activity, even at very high expression levels (data not shown). Most likely, mutation of MxA at residue Arg-408 not only prevents higher-order oligomerization but also disturbs a region that is essential for its antiviral function, and the L4 loop appears to be important for the interaction with the NP of IAV (8, 9, 12). Taken together, the data clearly demonstrate that dimeric as well as monomeric forms of MxA exhibited a pronounced antiviral activity, confirming that MxA assembly into higher-ordered oligomers is not a prerequisite for restricting IAV replication.

MxA Inhibits IAV Replication at a Step After Primary Transcription—We have shown previously that MxA inhibits replication of avian IAV in mouse cells at a cytoplasmic step following primary transcription of viral mRNAs (28). To verify that MxA also inhibits IAV replication in human cells at a step occurring after primary transcription, we infected cycloheximide-treated or untreated HEK293T cells expressing wild-type MxA, MxA(R640A), MxA(L617D), MxA(M527D), MxA(T103A), wild-type mouse Mx1 (mMx1), or the inactive mMx1(K49A) for 6 h with pH1N1-NP(H5N1) and performed RT qPCR analyses from isolated RNA with PB2-specific primers (Fig. 4*A*). mMx1 served as a positive control for the inhibition of primary transcription (Fig. 4*A*) (28). The data clearly show that, in cycloheximide-treated cells, wild-type MxA and MxA mutants forming complexes with defined stoichiometry did not affect primary transcription of IAV, whereas mouse Mx1, known to inhibit primary transcription, reduced the level of PB2 mRNA to less than 30%. As expected, the inactive Mx1(K49A) mutant exhibited no effect on the primary transcription of IAV. The activity of cycloheximide was verified in the same experiment by Western blotting (Fig. 4*B*). In the absence of cycloheximide, all antivirally active variants of MxA as well as mMx1 reduced the levels of PB2 mRNA to ~50% of the inactive controls MxA(T103A) and mMx1(K49A).

Next we monitored the nuclear import of IAV vRNPs into the nucleus of infected cells in the presence or absence of MxA expression. To make sure that no other IFN-induced effector protein was interfering with the assay, we utilized Vero cells lacking IFN type I genes. We infected Vero cells ectopically expressing wild-type MxA in the presence of cycloheximide with m.o.i. 10 of fowl plague virus (FPV, H7N7) and analyzed the nuclear import of vRNP by immunofluorescence microscopy using antibodies specific for IAV NP and MxA. FPV was chosen because of its high sensitivity to MxA (36) and efficient translocation of incoming vRNP into the nucleus.[5] As shown in Fig. 4, *C–E*, we were not able to detect any retention of the vRNPs in the cytoplasm when MxA was present. Images were assessed for nuclear import of vRNPs by counting MxA-expressing cells with a nuclear NP signal (Fig. 4*D*) or measuring the NP mean nuclear signal intensity of MxA-expressing cells (Fig. 4*E*). Cells transfected with empty vector were used as a negative control (Fig. 4, *D* and *E*). Taken together, these data demonstrate that human MxA does not interfere with the nuclear import of vRNPs and that it inhibits IAV replication at a step that follows primary transcription.

Overexpression of NP Interferes with the Antiviral Function of Human MxA—We and others have shown previously that overexpression of PB2 and NP interfered with the antiviral function of mouse Mx1 (15–17). Therefore, we next wanted to test whether the activity of MxA could be overcome by increased expression of NP and/or PB2. For this purpose, we

[5] P. E. Nigg and J. Pavlovic, unpublished data.

FIGURE 2. **Human MxA self-assembles into tetramers in the cytoplasm.** *A*, split GFP complementation assay with split-GFP-MxA fusion proteins in HeLa cells. Constructs encoding the indicated split-GFP-MxA fusion proteins were co-transfected. Twenty-four hours post-transfection, the cells were transferred to 27 °C, incubated for another 2 h, and fixated. MxA was immunostained with a mouse monoclonal antibody directed against MxA. Only dimeric or oligomeric forms of MxA yielded a GFP signal. The images shown are representative of three independent experiments. *w/o*, without. *B*, Western blot analysis of non-denaturing PAGE of lysates from Vero cells transiently transfected with plasmids encoding the indicated MxA variants or from A459 cells either stimulated with IFNα or left untreated. Immunostaining was performed with a rabbit polyclonal antibody directed against MxA. The molecular weights and the positions of the marker proteins used (nativeMARK, Invitrogen) are indicated. The Western blot shown is a representative of three independent experiments.

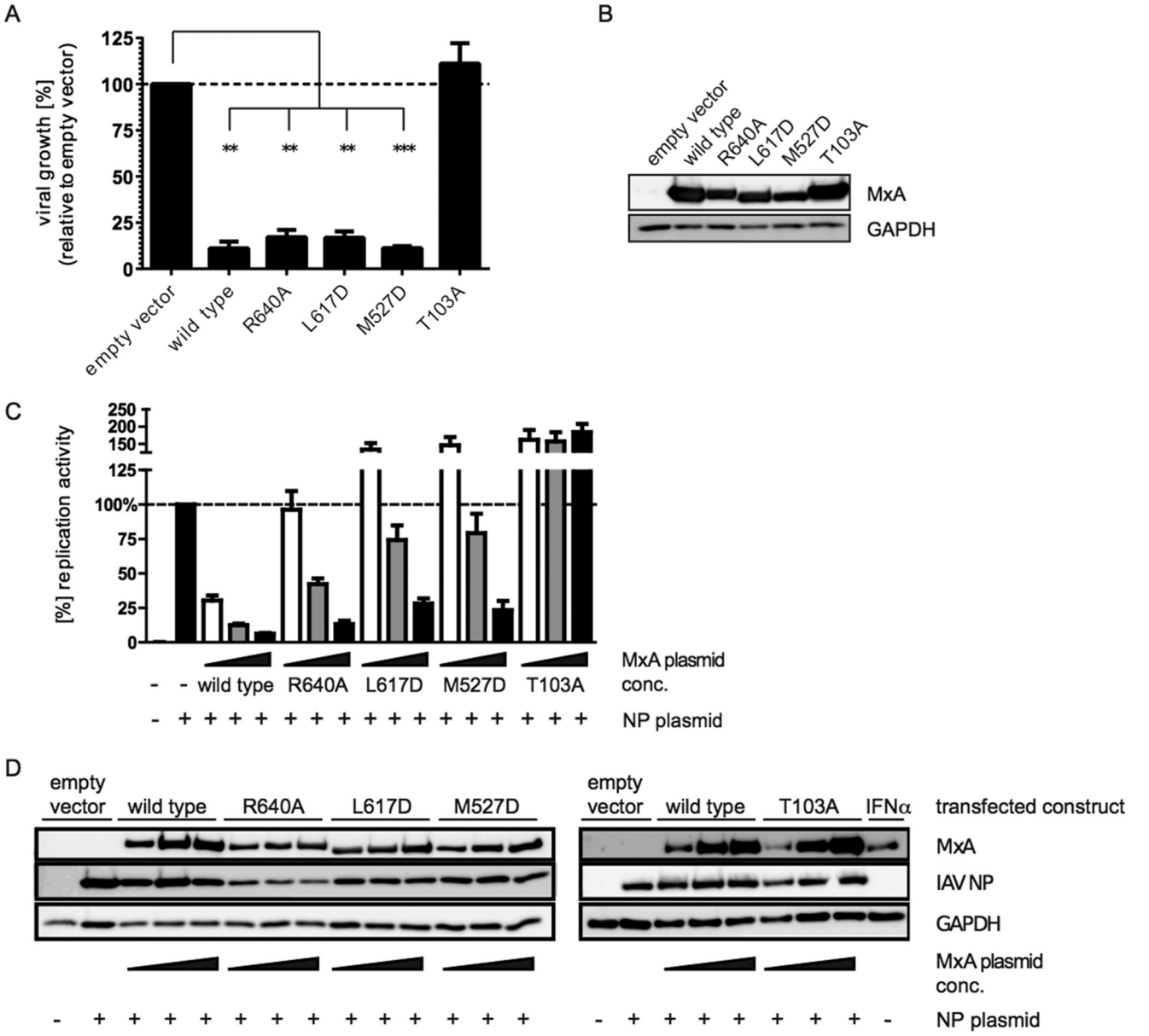

FIGURE 3. **MxA mutants with defined stoichiometry inhibit IAV replication.** *A*, HEK293T cells transiently expressing wild-type MxA or the indicated MxA mutants were infected with the IAV strain pH1N1-NP (H5N1) as detailed under "Experimental Procedures." Viral titers represented as $TCID_{50}$ per milliliter were determined directly on HEK293T cells expressing the indicated MxA mutants. $TCID_{50}$ per milliliter was determined from triplicates. *B*, Western blot analysis from lysates of cells expressing the indicated MxA variants used for viral titer determination shown in *A*. *C*, minimal replicon reconstitution assay. HEK293T cells were co-transfected with plasmids coding for the IAV proteins PB1, PB2, PA, and NP together with a reporter construct encoding firefly luciferase under the control of an IAV promoter and wild-type MxA or the indicated MxA mutants. Increasing amounts of plasmids encoding wild-type MxA or MxA mutants were added. *White columns*, 200 ng; *gray columns*, 400 ng; *black columns*, 800 ng. *A* and *C*, data are represented as mean ± S.E. of triplicates (Student's *t* test; **, $p < 0.05$). *D*, Western blot analysis of lysates from the minimal replicon reconstitution assays shown in *B*. Immunostaining was performed with antibodies directed against the indicated proteins. *IFNα*, control of endogenous MxA expressed in A549 cells in response to induction with IFNα; *conc.*, concentration.

made use of the IAV minimal replicon reconstitution assay in HEK293T cells either expressing wild-type MxA or the GTP binding-deficient mutant MxA(T103A). The level of wild-type MxA and MxA(T103A) expression was first adjusted to a level yielding ~50% to 70% inhibition of IAV polymerase activity by wild-type MxA compared with MxA(T103A) (Fig. 5, *A* and *B*). As a control, we employed mouse wild-type Mx1 and its inactive mutant Mx1(K49A) (Fig. 5, *C* and *D*). To assess whether NP or PB2 interferes with the MxA-mediated inhibition, gradually increasing amounts of plasmids encoding either PB2 (10–320 ng) or NP (50–1600 ng) were added to constant amounts of plasmids encoding MxA or MxA(T103A). To assess the interference of NP or PB2 with the activity of human MxA or mouse Mx1, the values (normalized for transfection efficiency) obtained for MxA or Mx1 were divided by the corresponding values for MxA(T103A) or Mx1(K49A) and expressed as percentage inhibition relative to the inactive mutants. For MxA, the results revealed that only increasing amounts of NP led to interference with the MxA activity, whereas increasing amounts of PB2 had no effect (Fig. 5, *A* and *B*). By contrast, overexpression of NP as well as PB2 interfered with the activity of mouse Mx1 (Fig. 5, *C* and *D*). Therefore, at least in this exper-

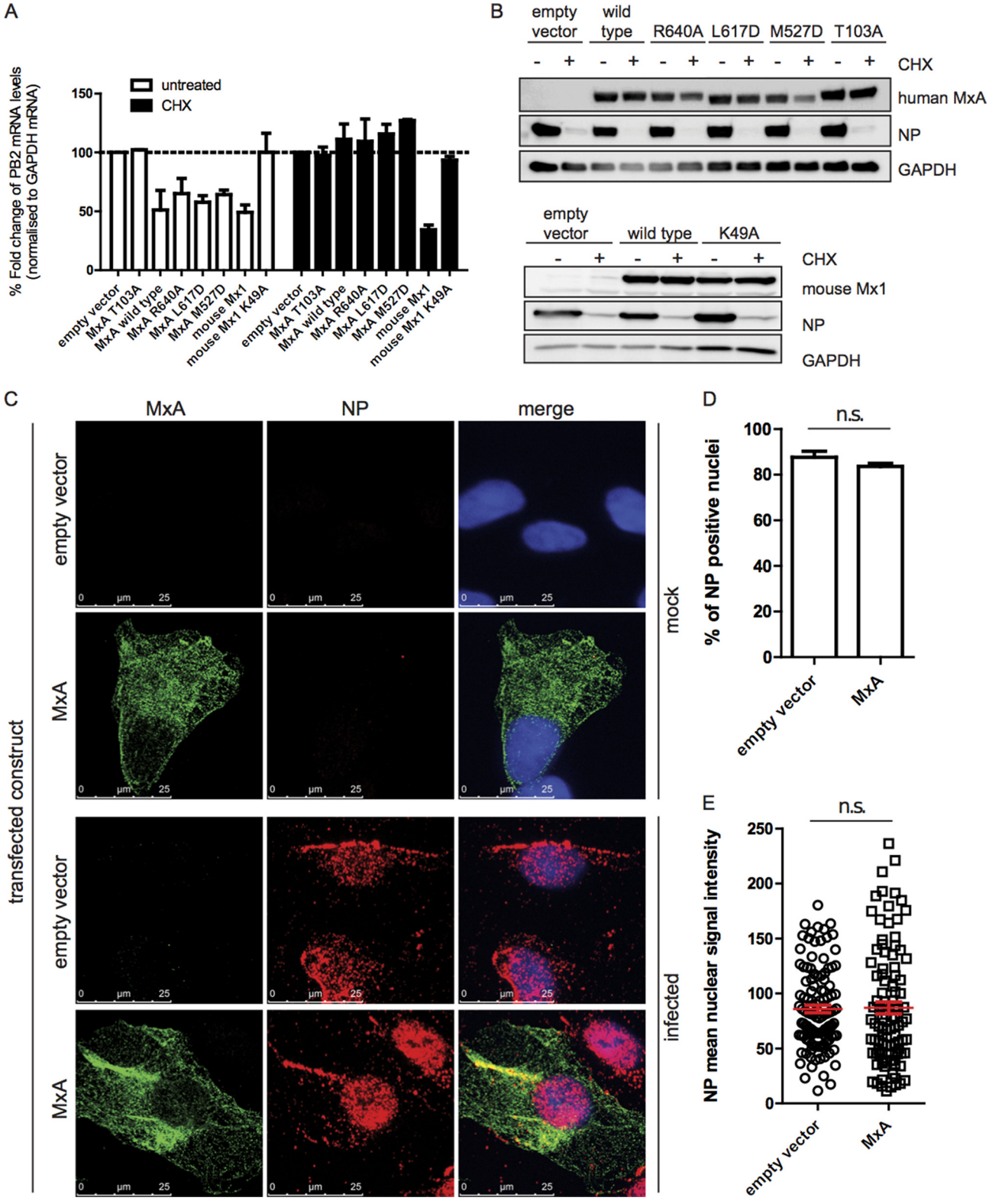

FIGURE 4. **MxA inhibits IAV replication at a step following primary transcription.** *A*, RT qPCR analysis of IAV PB2 mRNA in IAV pH1N1-NP-infected (H5N1) cells transiently expressing the indicated human MxA variants, mouse wild-type Mx1 (mMx1), or its inactive mutant Mx1(K49A). The cells were either treated with cycloheximide (*CHX*, *black columns*) or with EtOH as a solvent control (*white columns*). All experiments were performed in triplicate. The data are represented as mean ± S.E. *B*, Western blot analysis of lysates used for RT qPCR shown in *A*. Immunostaining was performed using antibodies directed against the indicated proteins. *C–E*, immunofluorescence analyses of nuclear import of incoming vRNPs. Vero cells transfected either with a plasmid encoding wild-type MxA or empty vector were infected with FPV (H7N7) in the presence of cycloheximide at 10 m.o.i. for 4 h. vRNPs and MxA were immunostained using antibodies directed against NP and MxA. *C*, confocal laser-scanning microscopy images. *Red*, NP; *green*, MxA; *blue*, DAPI. Shown are representative images. The experiment was performed in biological duplicates. 50 cells/replicate were recorded. *D*, nuclear import of vRNPs was assessed by counting NP-positive nuclei of images recorded in *C*. *n.s.*, not significant. *E*, quantification of vRNP import by NP mean nuclear signal intensity of images recorded in *C*. The data are represented as mean ± S.E. *D* and *E*, Student's *t* test, $p < 0.05$.

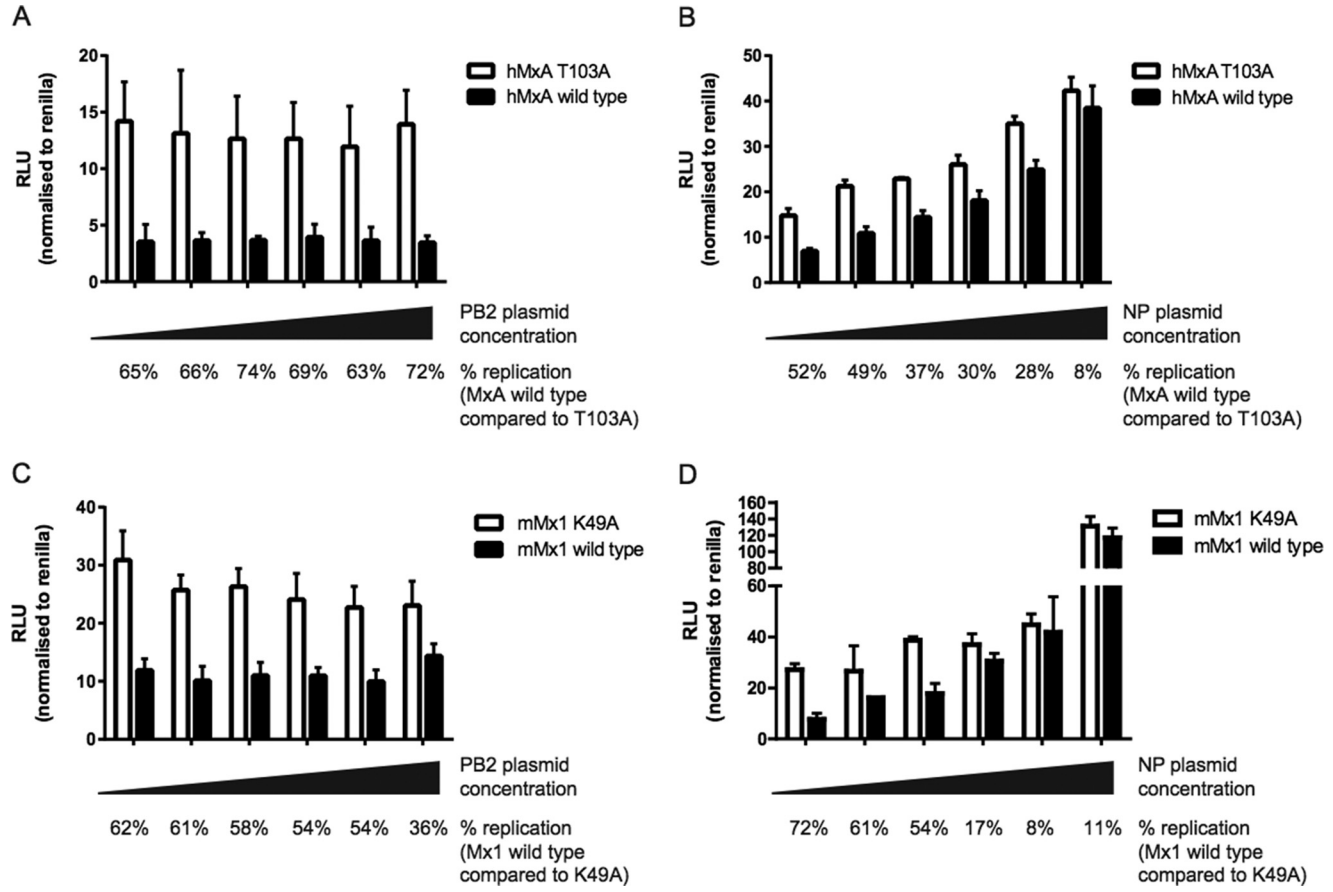

FIGURE 5. **Overexpression of NP but not PB2 interferes with the antiviral activity of MxA.** *A* and *B*, plasmids encoding wild-type MxA or the inactive mutant MxA(T103A) were co-transfected with increasing amounts of plasmids encoding (*A*) PB2 (10, 20, 40, 80, 160, or 320 ng) or (*B*) NP (50, 100, 200, 400, 800, or 1600 ng) together with the plasmids of the minimal replicon reconstitution assay derived from an H5N1 virus. *RLU*, relative light units. *C* and *D*, plasmids encoding wild-type mouse Mx1 or Mx1(K49A) were co-transfected with increasing amounts of plasmids encoding PB2 (*C*) or NP (*D*) (see *A* and *B*) together with the plasmids of the minimal replicon reconstitution assay derived from an H5N1 virus. The number given below each column pair represents the percentage of inhibition of the polymerase activity by wild-type MxA or Mx1 compared with the corresponding values in the presence of the respective inactive mutant, MxA(T103A) or Mx1(K49A). The experiment was performed in biological triplicates, and the data are represented as mean ± S.E.

imental setup, MxA appeared to target only NP, whereas Mx1 appeared to functionally interact with both NP and PB2, as described previously. The increased values obtained in samples with a high concentration of NP independent of MxA or Mx1 are the result of enhanced replication efficiency of the mini replicon (Fig. 5, *B* and *D*) in the presence of a high concentration of NP.

Dimeric Variants of MxA Interact with NP Independent of Other Viral Proteins—Despite the fact that, so far, experimental evidence for a physical interaction of human MxA with NP is lacking, the available data strongly suggest a functional relationship between these two proteins (18, 19, 33) (Fig. 5*B*). On the basis of our observations that GTP binding led to a disassembly of MxA from higher-ordered oligomers to tetramers and dimers that efficiently blocked IAV replication, we wanted to test whether MxA variants forming complexes with defined stoichiometry would exhibit a higher affinity to NP than wild-type MxA. For this purpose, we carried out co-immunoprecipitation assays. We transfected Vero cells with plasmids encoding wild-type MxA, MxA(R640A), MxA(L617D), MxA(M527D), or MxA(T103A) and subsequently infected them for 6 h with the IAV strains pH1N1-NP(H5N1) or rSC35M, both highly sensitive to the activity of MxA. Immunoprecipitation of NP revealed that both dimer-forming variants, the hinge 1 mutant MxA(R640A), as well as the interface mutant MxA(L617D) efficiently co-precipitated with NP. Wild-type MxA, the monomeric variant MxA(M527D), and the GTP binding-deficient mutant MxA(T103A) exhibited no or only a barely detectable interaction with NP (Fig. 6*A*). Therefore, these data strongly support our model that oligomeric MxA has first to be converted into dimers to efficiently bind to NP. Because NP exists in a vRNP-bound form as well as in an unbound form in infected cells, we assessed in a next step whether MxA is able to interact with ectopically expressed NP in the absence of any additional viral component. Therefore, we co-transfected plasmids encoding wild-type MxA, MxA(R640A), MxA(L617D), MxA(M527D), or MxA(T103A) with plasmids encoding NP either derived from a highly Mx-sensitive avian IAV strain (Kan-1) or two MxA-resistant strains (A/Hamburg/4/2009 (pH1N1) and A/PR/8/34 strain (PR8)). The NP of the MxA-sensitive strain efficiently co-precipitated with the two dimeric variants of MxA (Fig. 6*B*), corroborating the findings observed with IAV infection (Fig. 6*A*). We also observed co-immunoprecipitation of dimeric forms of MxA with NP of the MxA-resistant strains p(H1N1) and PR8, although to a lesser extent than with the NP of Kan-1 (Fig. 6*B*).

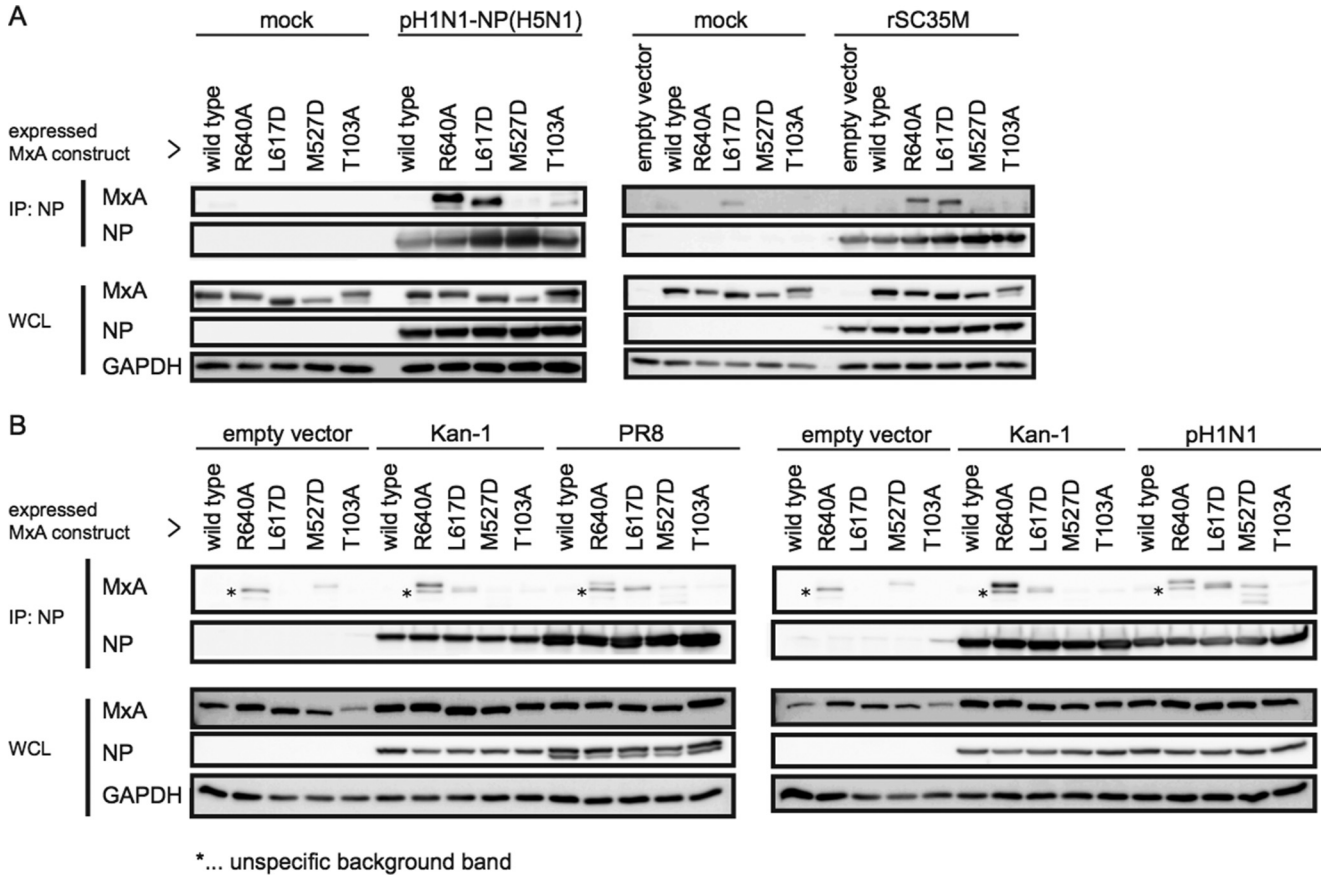

FIGURE 6. **Dimeric forms of MxA form stable complexes with NP.** *A*, Vero cells were transfected with plasmids encoding the indicated MxA variants and then infected for 6 h with m.o.i. 5 of IAV strain pH1N1-NP(H5N1) (*left panel*) or IAV strain rSC35M (*right panel*). NP was immunoprecipitated (*IP*) from lysates using a mouse monoclonal NP-specific antibody, and the resulting complexes were subjected to Western blot analyses using polyclonal rabbit antibodies specific for MxA and NP. In addition, input samples (whole cell lysates, *WCL*) also were monitored for expression of MxA, NP, and GAPDH (loading control) by Western blot analysis. *B*, Vero cells were co-transfected with plasmids encoding the indicated MxA variants together with plasmids encoding NP from the indicated IAV strains. Immunoprecipitation of NP and Western blot analyses of immunoprecipitated proteins and whole cell lysates were performed as described in *A*. Immunostaining of the Western blots was performed with antibodies against MxA, NP, or GAPDH. The Western blots shown are representative of three independent experiments.

Discussion

The human MxA protein restricts the replication of a broad variety of negative- and positive-stranded RNA viruses as well as DNA viruses. Besides their different genomes, these viruses replicate at different subcellular locations, employing different replication strategies. Therefore, MxA either interferes with viral replication via a general, rather nonspecific mechanism affecting many different viruses, or MxA has developed different molecular mechanisms to block virus replication. Although, for some viruses, such as IAV, Thogotovirus, and La Crosse virus, the replication steps and/or viral targets inhibited by MxA have been identified, for most MxA-restricted viruses the mode of action or the viral targets remain undetermined.

Using murine 3T3 cells, we have shown previously that MxA inhibits IAV replication at a step occurring after primary transcription. Synthesis of primary transcripts of the polymerase subunits, hemaglutinin, neuraminidase, and NP are unaffected by MxA, whereas, surprisingly, the production of primary transcripts of NS1 and M1 is increased 2- to 3-fold. The primary transcripts are exported efficiently and have the capacity to be translated *in vitro* (28). However, when translocated to the nucleus by means of an N-terminal nuclear localization sequence, MxA efficiently blocks primary transcription of IAV (7). We now observed very similar results in human cells. Ectopic expression of MxA restricted IAV replication without affecting the nuclear import of incoming vRNPs (Fig. 4). In addition, our RT qPCR data obtained from mRNA isolated from HEK293T MxA-expressing cells infected with IAV revealed that, in the presence of MxA, primary transcription of PB2 mRNA is not blocked (Fig. 4*A*). Xiao *et al.* (39) have reported recently that MxA interferes with IAV replication at two distinct stages, a step prior to primary transcription together with an unknown IFN-induced protein and a step following primary transcription. In our study, we focused only on the second step and analyzed the antiviral function of MxA in the absence of other IFN-induced effector proteins known to inhibit IAV entry and uncoating, such as IFITMs (40).

Mx proteins have the capacity to assemble into oligomeric structures of various complexities. *In vitro*, MxA protein assembles into tetramers (12) and has the capacity to assume higher-ordered oligomeric structures by forming rings or helical filaments (41, 42). Moreover, on the basis of the crystal structure, Gao *et al.* (5, 12) have proposed that MxA assembles into ring-like structures. The question whether monomeric

and/or oligomeric forms of MxA exert their antiviral activity against IAV and other viruses remains an unsolved issue. Several previous studies have demonstrated that the monomeric mutant MxA(L612K) efficiently restricts IAV, Thogotovirus, and vesicular stomatitis virus (6, 25, 27). However, Gao *et al.* (5, 12) have reported recently that dimeric and monomeric interface and hinge mutants of MxA failed to exhibit antiviral activity against IAV and La Crosse virus using a minimal replicon reconstitution assay for IAV or an N sequestration assay for La Crosse virus, respectively. On the basis of their findings, Gao *et al.* (5) have proposed a model in which MxA would assemble into oligomeric rings around incoming vRNPs of IAV. The major caveat of this model, however, is the fact that MxA inhibits IAV replication after the nuclear import of viral RNPs and after primary transcription of viral mRNAs has taken place (Fig. 4) (7, 28). Therefore, we re-evaluated the antiviral activity of the dimeric and monomeric variants of MxA (plasmids provided by Georg Kochs) by performing infection experiments with IAV. Intriguingly, dimeric MxA variants with mutations in the stalk interface 1 or BSE hinge region as well as the monomeric interface 2 mutant efficiently restricted IAV, indicating that MxA does not necessarily have to assemble into higher oligomeric structures to exert antiviral activity against IAV. On the basis of the same minimal replicon reconstitution assay we used in this study (Fig. 3*C*), Gao *et al.* (5, 12) have shown previously that the MxA variants forming complexes with defined stoichiometry, MxA(R640A), MxA(L617D), and MxA(M527D), do not restrict IAV replication. However, they adjusted the amount of MxA expression to a level where wild-type MxA only reduced the activity of the IAV polymerase complex to 70–80% of the negative control. In fact, we obtained very similar results at low expression levels of MxA proteins (Fig. 3*C*).

The question of whether GTP promotes oligomerization or disassembly of MxA oligomers remains an issue of debate. Clearly, oligomerization of purified MxA is highly salt-dependent (41). Here we observed that, in the absence of GTP under medium salt conditions (200 mM KCl), purified recombinant MxA formed higher-order oligomers that, upon addition of GTPγS, disassembled primarily into tetramers and, to a lower extent, also into dimers. Similarly, Kochs *et al.* (41) have demonstrated previously that, under high-salt conditions (300 mM NaCl), MxA exists predominantly in a lower oligomeric, non-sedimentable form. Addition of GTPγS does not increase the sedimentable fraction of MxA, indicating that GTPγS does not mediate oligomerization. By contrast, Gao *et al.* (5, 12) have reported recently that, under the same experimental conditions, the non-sedimentable fraction of MxA converts into a sedimentable oligomeric structure. The authors explained their observation with the generation of an additional nucleotide-dependent interphase in the G domain (5). However, recent evidence indicates that GTP-dependent G domain dimerization of MxA is a transient process that cannot be stabilized by GTPγS (13). Under low-salt conditions, MxA forms predominantly condensed oligomeric and sedimentable structures that, in the presence of GTPγS, rearrange into spiral or stack-like forms (41). In the case of dynamin, preassembled sedimentable oligomers convert into lower oligomeric, non-sedimentable structures in the presence of GTPγS (37).

In vitro, the hinge 1 mutant MxA(R640A) predominantly formed tetramers that converted into dimers in the presence of GTPγS (Fig. 1*B*). Gao *et al.* (5) have purified recombinant MxA(R640A) predominantly in the form of dimers, even in the absence of GTPγS, but in the presence of substantially higher salt concentrations (400 mM) . Therefore, it is conceivable that, for MxA(R640A) like for wild-type MxA, the stoichiometry of these recombinant proteins is not only a function of GTP but also strongly dependent on salt concentration.

Non-denaturing PAGE analyses of MxA expressed endogenously or ectopically in human cells revealed that wild-type MxA accumulated primarily in a tetrameric form. The reason why MxA(R640A), in our hands, runs predominantly as a tetramer when affinity-purified but as a dimer when analyzed in lysates of mammalian cells is not entirely clear, but it might be due to the presence of GTP and/or accessory proteins in the cellular context. Taken together, wild-type MxA appears to exist primarily as tetramer in the cytoplasm of infected cells and, at least *in vitro*, has the capacity to disassemble into dimers in a GTP-dependent fashion. The fact that the dimeric forms MxA(R640A) and MxA(L617D) exert antiviral activity strongly suggests that the GTP-dependent formation of dimers is important for the function of MxA. In this context, it is interesting to note that human MxB (Mx2), shown recently to restrict human immunodeficiency virus, appears to act as a dimer, albeit in a GTP-independent manner (43–45).

The observation that predominantly dimeric forms of MxA have the capacity form stable complexes with NP in infected cells lends further support to our hypothesis that dimers play a pivotal role for the activity of MxA. The fact that MxA dimers also formed a complex with ectopically expressed NP from a highly Mx-sensitive avian H5N1 strain in the absence of any other viral component demonstrates that MxA can interact with NP that is not bound within the vRNP. Wild-type MxA did not form a complex with NP at detectable levels, even when the cells were infected with a highly MxA-sensitive virus (Fig. 6*A*). A possible explanation for this observation may be that, following infection with IAV, only small amounts of MxA are disassembled into dimers to interact with NP. The major part of MxA could then remain in higher-ordered oligomeric structures. Alternatively, it may be possible that the high affinity of the MxA dimer to NP is only required for the initial recognition of NP. After the initial interaction, MxA could convert again into higher oligomeric structures exhibiting a low affinity for NP. *In vitro* NP is known to form oligomers even in the absence of RNA (46). Therefore, it may be possible that MxA reoligomerizes around newly synthesized NP oligomers, thereby inhibiting its function. In the case of the antivirally active monomeric form of MxA, MxA(M527D), it is conceivable that a low-affinity interaction to NP is sufficient for antiviral activity in certain assays. Alternatively, the transient G domain dimerization stimulated by GTP binding (13) could also result in a transiently increased affinity for NP that may be sufficient to disrupt binding of NP to UAP56.

Testing the interaction of NPs from two distinct MxA-resistant strains revealed that NP from the 2009 pandemic H1N1 strain (pH1N1) was still capable of interacting with MxA, whereas NP from the PR8 strain (a derivative of the 1918 H1N1

strain) showed reduced complex formation. Interestingly, these two IAV strains developed their MxA resistance phenotype independently of each other (19) and, therefore, introduced distinct adaptive mutations into their NP coding sequence. These findings led us to the conclusion that there are at least two mechanisms for IAV to evade restriction by MxA. For the PR8 strain, this entails minimizing the affinity to MxA, whereas the pH1N1 strain employed a different strategy, possibly by reducing the affinity to an MxA-associated protein such as UAP56 (30).

Whether MxA interacts directly with NP or via the MxA-associated UAP56 remains to be determined. Of course, it is possible that MxA restricts the replication of viruses other than IAV by oligomerizing into ring-like structures around nucleocapsids, "strangling" them in a dynamin-like fashion by GTP-dependent mechanical constriction (13). However, on the basis of our data presented here, we propose a new model in which, in response to IFN induction, MxA is synthesized and assembled into higher oligomeric structures, possibly partially associated with membranes of the smooth endoplasmic reticulum (38). These oligomeric structures may represent a preactive form of MxA. In infected cells, a still undefined viral component would then trigger a GTP-driven disassembly of oligomeric MxA into dimers, allowing the association with newly synthesized NP translated from primary transcripts. Therefore, sequestration of NP from replication sites in the nucleus may represent the long sought after mechanism of MxA action against IAV.

Author Contributions—J. P. conceived the study and wrote the paper. P. E. N. designed, performed, and analyzed all experiments. Both authors reviewed the results and approved the final version of the manuscript.

Acknowledgments—We thank Georg Kochs for the interface and hinge constructs of MxA. We also thank Eva Moritz for technical support and Birgit Dreier for help with the MALS assays and Ben Hale, Otto Haller, Peter Staeheli, Georg Kochs, Dominik Müller, Fiona Steiner, and Michel Crameri for critical reading of the manuscript.

References

1. Der, S. D., Zhou, A., Williams, B. R., and Silverman, R. H. (1998) Identification of genes differentially regulated by interferon α, β, or γ using oligonucleotide arrays. *Proc. Natl. Acad. Sci. U.S.A.* **95,** 15623–15628
2. de Veer, M. J., Holko, M., Frevel, M., Walker, E., Der, S., Paranjape, J. M., Silverman, R. H., and Williams, B. R. (2001) Functional classification of interferon-stimulated genes identified using microarrays. *J. Leukocyte Biol.* **69,** 912–920
3. Samarajiwa, S. A., Forster, S., Auchettl, K., and Hertzog, P. J. (2009) INTERFEROME: the database of interferon regulated genes. *Nucleic Acids Res.* **37,** D852–857
4. Haller, O., and Kochs, G. (2011) Human MxA protein: an interferon-induced dynamin-like GTPase with broad antiviral activity. *J. Interferon Cytokine Res.* **31,** 79–87
5. Gao, S., von der Malsburg, A., Dick, A., Faelber, K., Schröder, G. F., Haller, O., Kochs, G., and Daumke, O. (2011) Structure of myxovirus resistance protein a reveals intra- and intermolecular domain interactions required for the antiviral function. *Immunity* **35,** 514–525
6. Di Paolo, C., Hefti, H. P., Meli, M., Landis, H., and Pavlovic, J. (1999) Intramolecular backfolding of the carboxyl-terminal end of MxA protein is a prerequisite for its oligomerization. *J. Biol. Chem.* **274,** 32071–32078
7. Zürcher, T., Pavlovic, J., and Staeheli, P. (1992) Mechanism of human MxA protein action: variants with changed antiviral properties. *EMBO J.* **11,** 1657–1661
8. Patzina, C., Haller, O., and Kochs, G. (2014) Structural requirements for the antiviral activity of the human MxA protein against Thogoto and influenza A virus. *J. Biol. Chem.* **289,** 6020–6027
9. Mitchell, P. S., Patzina, C., Emerman, M., Haller, O., Malik, H. S., and Kochs, G. (2012) Evolution-guided identification of antiviral specificity determinants in the broadly acting interferon-induced innate immunity factor MxA. *Cell Host Microbe* **12,** 598–604
10. Chappie, J. S., Acharya, S., Liu, Y. W., Leonard, M., Pucadyil, T. J., and Schmid, S. L. (2009) An intramolecular signaling element that modulates dynamin function *in vitro* and *in vivo*. *Mol. Biol. Cell* **20,** 3561–3571
11. Pitossi, F., Blank, A., Schröder, A., Schwarz, A., Hüssi, P., Schwemmle, M., Pavlovic, J., and Staeheli, P. (1993) A functional GTP-binding motif is necessary for antiviral activity of Mx proteins. *J. Virol.* **67,** 6726–6732
12. Gao, S., von der Malsburg, A., Paeschke, S., Behlke, J., Haller, O., Kochs, G., and Daumke, O. (2010) Structural basis of oligomerization in the stalk region of dynamin-like MxA. *Nature* **465,** 502–506
13. Rennie, M. L., McKelvie, S. A., Bulloch, E. M., and Kingston, R. L. (2014) Transient dimerization of human MxA promotes GTP hydrolysis, resulting in a mechanical power stroke. *Structure* **22,** 1433–1445
14. Schwemmle, M., Weining, K. C., Richter, M. F., Schumacher, B., and Staeheli, P. (1995) Vesicular stomatitis virus transcription inhibited by purified MxA protein. *Virology* **206,** 545–554
15. Stranden, A. M., Staeheli, P., and Pavlovic, J. (1993) Function of the mouse Mx1 protein is inhibited by overexpression of the Pb2 protein of influenza-virus. *Virology* **197,** 642–651
16. Verhelst, J., Parthoens, E., Schepens, B., Fiers, W., and Saelens, X. (2012) Interferon-inducible protein Mx1 inhibits influenza virus by interfering with functional viral ribonucleoprotein complex assembly. *J. Virol.* **86,** 13445–13455
17. Huang, T., Pavlovic, J., Staeheli, P., and Krystal, M. (1992) Overexpression of the influenza virus polymerase can titrate out inhibition by the murine Mx1 protein. *J. Virol.* **66,** 4154–4160
18. Zimmermann, P., Mänz, B., Haller, O., Schwemmle, M., and Kochs, G. (2011) The viral nucleoprotein determines Mx sensitivity of influenza A viruses. *J. Virol.* **85,** 8133–8140
19. Mänz, B., Dornfeld, D., Götz, V., Zell, R., Zimmermann, P., Haller, O., Kochs, G., and Schwemmle, M. (2013) Pandemic influenza A viruses escape from restriction by human MxA through adaptive mutations in the nucleoprotein. *PLoS Pathog.* **9,** e1003279
20. Riegger, D., Hai, R., Dornfeld, D., Mänz, B., Leyva-Grado, V., Sánchez-Aparicio, M. T., Albrecht, R. A., Palese, P., Haller, O., Schwemmle, M., García-Sastre, A., Kochs, G., and Schmolke, M. (2015) The nucleoprotein of newly emerged H7N9 influenza A virus harbors a unique motif conferring resistance to antiviral human MxA. *J. Virol.* **89,** 2241–2252
21. Turan, K., Mibayashi, M., Sugiyama, K., Saito, S., Numajiri, A., and Nagata, K. (2004) Nuclear MxA proteins form a complex with influenza virus NP and inhibit the transcription of the engineered influenza virus genome. *Nucleic Acids Res.* **32,** 643–652
22. Momose, F., Basler, C. F., O'Neill, R. E., Iwamatsu, A., Palese, P., and Nagata, K. (2001) Cellular splicing factor RAF-2p48/NPI-5/BAT1/UAP56 interacts with the influenza virus nucleoprotein and enhances viral RNA synthesis. *J. Virol.* **75,** 1899–1908
23. Read, E. K., and Digard, P. (2010) Individual influenza A virus mRNAs show differential dependence on cellular NXF1/TAP for their nuclear export. *J. Gen. Virol.* **91,** 1290–1301
24. Wisskirchen, C., Ludersdorfer, T. H., Müller, D. A., Moritz, E., and Pavlovic, J. (2011) The cellular RNA helicase UAP56 is required for prevention of double-stranded RNA formation during influenza A virus infection. *J. Virol.* **85,** 8646–8655
25. Schumacher, B., and Staeheli, P. (1998) Domains mediating intramolecular folding and oligomerization of MxA GTPase. *J. Biol. Chem.* **273,** 28365–28370
26. Ponten, A., Sick, C., Weeber, M., Haller, O., and Kochs, G. (1997) Dominant-negative mutants of human MxA protein: domains in the carboxy-terminal moiety are important for oligomerization and antiviral activity. *J. Virol.* **71,** 2591–2599
27. Janzen, C., Kochs, G., and Haller, O. (2000) A monomeric GTPase-nega-

tive MxA mutant with antiviral activity. *J. Virol.* **74,** 8202–8206
28. Pavlovic, J., Haller, O., and Staeheli, P. (1992) Human and mouse Mx proteins inhibit different steps of the influenza virus multiplication cycle. *J. Virol.* **66,** 2564–2569
29. Aebi, M., Fäh, J., Hurt, N., Samuel, C. E., Thomis, D., Bazzigher, L., Pavlovic, J., Haller, O., and Staeheli, P. (1989) cDNA structures and regulation of two interferon-induced human Mx proteins. *Mol. Cell Biol.* **9,** 5062–5072
30. Wisskirchen, C., Ludersdorfer, T. H., Müller, D. A., Moritz, E., and Pavlovic, J. (2011) Interferon-induced antiviral protein MxA interacts with the cellular RNA helicases UAP56 and URH49. *J. Biol. Chem.* **286,** 34743–34751
31. Walker, J. M. (1994) Nondenaturing polyacrylamide gel electrophoresis of proteins. *Methods Mol. Biol.* **32,** 17–22
32. Fiala, G. J., Schamel, W. W., and Blumenthal, B. (2011) Blue native polyacrylamide gel electrophoresis (BN-PAGE) for analysis of multiprotein complexes from cellular lysates. *J. Vis. Exp.* **48,** e2164
33. Dittmann, J., Stertz, S., Grimm, D., Steel, J., García-Sastre, A., Haller, O., and Kochs, G. (2008) Influenza A virus strains differ in sensitivity to the antiviral action of Mx-GTPase. *J. Virol.* **82,** 3624–3631
34. Pfaffl, M. W. (2001) A new mathematical model for relative quantification in real-time RT-PCR. *Nucleic Acids Res.* **29,** e45
35. Schneider-Schaulies, S., Schneider-Schaulies, J., Schuster, A., Bayer, M., Pavlovic, J., and ter Meulen, V. (1994) Cell type-specific MxA-mediated inhibition of measles virus transcription in human brain cells. *J. Virol.* **68,** 6910–6917
36. Pavlovic, J., Zürcher, T., Haller, O., and Staeheli, P. (1990) Resistance to influenza virus and vesicular stomatitis virus conferred by expression of human MxA protein. *J. Virol.* **64,** 3370–3375
37. Warnock, D. E., Hinshaw, J. E., and Schmid, S. L. (1996) Dynamin self-assembly stimulates its GTPase activity. *J. Biol. Chem.* **271,** 22310–22314
38. Stertz, S., Reichelt, M., Krijnse-Locker, J., Mackenzie, J., Simpson, J. C., Haller, O., and Kochs, G. (2006) Interferon-induced, antiviral human MxA protein localizes to a distinct subcompartment of the smooth endoplasmic reticulum. *J. Interferon Cytokine Res.* **26,** 650–660
39. Xiao, H., Killip, M. J., Staeheli, P., Randall, R. E., and Jackson, D. (2013) The human interferon-induced MxA protein inhibits early stages of influenza A virus infection by retaining the incoming viral genome in the cytoplasm. *J. Virol.* **87,** 13053–13058
40. Brass, A. L., Huang, I. C., Benita, Y., John, S. P., Krishnan, M. N., Feeley, E. M., Ryan, B. J., Weyer, J. L., van der Weyden, L., Fikrig, E., Adams, D. J., Xavier, R. J., Farzan, M., and Elledge, S. J. (2009) The IFITM proteins mediate cellular resistance to influenza A H1N1 virus, West Nile virus, and dengue virus. *Cell* **139,** 1243–1254
41. Kochs, G., Haener, M., Aebi, U., and Haller, O. (2002) Self-assembly of human MxA GTPase into highly ordered dynamin-like oligomers. *J. Biol. Chem.* **277,** 14172–14176
42. Accola, M. A., Huang, B., Al Masri, A., and McNiven, M. A. (2002) The antiviral dynamin family member, MxA, tubulates lipids and localizes to the smooth endoplasmic reticulum. *J. Biol. Chem.* **277,** 21829–21835
43. Goujon, C., Moncorgé, O., Bauby, H., Doyle, T., Ward, C. C., Schaller, T., Hué, S., Barclay, W. S., Schulz, R., and Malim, M. H. (2013) Human MX2 is an interferon-induced post-entry inhibitor of HIV-1 infection. *Nature* **502,** 559–562
44. Fribourgh, J. L., Nguyen, H. C., Matreyek, K. A., Alvarez, F. J., Summers, B. J., Dewdney, T. G., Aiken, C., Zhang, P., Engelman, A., and Xiong, Y. (2014) Structural insight into HIV-1 restriction by MxB. *Cell Host Microbe* **16,** 627–638
45. Dicks, M. D., Goujon, C., Pollpeter, D., Betancor, G., Apolonia, L., Bergeron, J. R., and Malim, M. H. (2015) Oligomerization requirements for MX2 mediated suppression of HIV-1 infection. *J. Virol.* 10.1128/JVI.02247-15
46. Tarus, B., Bakowiez, O., Chenavas, S., Duchemin, L., Estrozi, L. F., Bourdieu, C., Lejal, N., Bernard, J., Moudjou, M., Chevalier, C., Delmas, B., Ruigrok, R. W., Di Primo, C., and Slama-Schwok, A. (2012) Oligomerization paths of the nucleoprotein of influenza A virus. *Biochimie* **94,** 776–785
47. Reed, L. J., and Muench, H. (1938) A simple method of estimating fifty percent endpoints. *Am. J. Hyg.* **27,** 493–497

Oligomerization and GTP-binding Requirements of MxA for Viral Target Recognition and Antiviral Activity against Influenza A Virus

Patricia E. Nigg and Jovan Pavlovic

J. Biol. Chem. 2015, 290:29893-29906.
doi: 10.1074/jbc.M115.681494 originally published online October 27, 2015
